JACS
JOURNAL OF THE AMERICAN CHEMICAL SOCIETY

ARTICLE

pubs.acs.org/JACS

Design Parameters for Tuning the Type 1 Cu Multicopper Oxidase Redox Potential: Insight from a Combination of First Principles and Empirical Molecular Dynamics Simulations

Gongyi Hong,[†,‡] Dmitri M. Ivnitski,[§] Glenn R. Johnson,[∥] Plamen Atanassov,[§] and Ruth Pachter[†,*]

[†]Air Force Research Laboratory, Materials & Manufacturing Directorate, Wright-Patterson Air Force Base, Ohio 45433, United States

[‡]General Dynamics Information Technology, Inc. and [§]Chemical & Nuclear Engineering Department, University of New Mexico, Albuquerque, New Mexico 87131, United States

[∥]Air Force Research Laboratory, Materials & Manufacturing Directorate, Tyndall Air Force Base, Florida 3240, United States

Supporting Information

ABSTRACT: The redox potentials and reorganization energies of the type 1 (T1) Cu site in four multicopper oxidases were calculated by combining first principles density functional theory (QM) and QM/MM molecular dynamics (MD) simulations. The model enzymes selected included the laccase from *Trametes versicolor*, the laccase-like enzyme isolated from *Bacillus subtilis*, CueO required for copper homeostasis in *Escherichia coli*, and the small laccase (SLAC) from *Streptomyces coelicolor*. The results demonstrated good agreement with experimental data and provided insight into the parameters that influence the T1 redox potential. Effects of the immediate T1 Cu site environment, including the His(N_δ)-Cys(S)-His(N_δ) and the axial coordinating amino acid, as well as the proximate $H(N)_{backbone}-S_{Cys}$ hydrogen bond, were discerned. Furthermore, effects of the protein backbone and side-chains, as well as of the aqueous solvent, were studied by QM/MM molecular dynamics (MD) simulations, providing an understanding of influences beyond the T1 Cu coordination sphere. Suggestions were made regarding an increase of the T1 redox potential in SLAC, i.e., of Met198 and Thr232 in addition to the axial amino acid Met298. Finally, the results of this work presented a framework for understanding parameters that influence the Type 1 Cu MCO redox potential, useful for an ever-growing range of laccase-based applications.

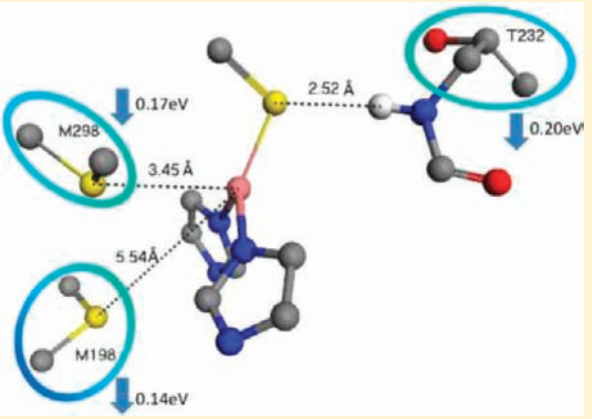

INTRODUCTION

Multicopper oxidases (MCOs) have been widely examined due to their ability to couple the oxidation of a range of aromatic substrates to the catalytic reduction of molecular oxygen to yield water. Properties of laccases, L-ascorbate oxidase, ceruloplasmin, bilirubin oxidase, and phenoxazinone synthase, were extensively reviewed (refs 1 and 2 and references therein). Properties of the redox-active copper atoms have been described, including, for example, absorption characteristics,[3] electron transfer,[1,4,5] molecular structure,[6] and the thermodynamic parameters of the so-called type 1 (T1) Cu site.[7] In addition, substrate oxidation as a function of the T1 Cu redox potential[8] has also been investigated. Notably, laccases represent the largest subgroup of MCOs, with many examples isolated from fungal[9] and bacterial[10] backgrounds.[11] The nature of the laccases' molecular structure, catalytic mechanisms, and expression, were reviewed in detail by Giardina et al.,[2] highlighting the enzymes' utility for a variety of processes in biotechnological applications. For example, fungal laccases have an exceptionally broad substrate preference and are growing in importance for environmentally-friendly synthesis. Applications include production of new antibiotics, enzymatic derivatization of amino acids, preparation of polymeric complexes, synthesis of heteropolymeric adhesives, among other examples, recently further reported (ref 12 and references therein). As pointed out, hundreds of aromatic substrates are known to be transformed by laccases, and could be further enhanced by mediator systems. Effective enzyme immobilization has been shown to improve laccase-based applications, leading to increased enzyme stability and improved resistance to pH and temperature changes.[12] Enzymatic delignification is also of growing interest, as lignin removal is a central issue in paper and pulp industries. Laccase-mediator systems, generally needed because laccases have relatively low redox potentials, commercialized in several sectors (including textile), could be applied for delignification.[13] However, at the same time, challenges in applying MCOs were

Received: June 25, 2010
Published: March 09, 2011

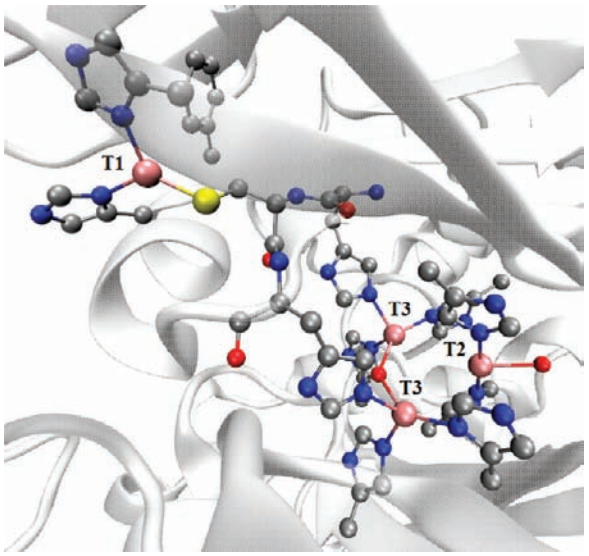

Figure 1. T1, T2, and T3 Cu sites in TvL, from the X-ray crystal structure.[14]

pointed out by Rodgers et al.,[1] as well as recommendations to address them. A better understanding of structure−function relationships, particularly regarding the T1 Cu potential, which will enable rational mutagenesis, is of importance.

Copper centers in MCOs have conserved active sites, consisting of the T1 Cu site (see, for example, Figure 1, from the X-ray structure of *Trametes versicolor* laccase (TvL),[14] assuming a distorted tetrahedral coordination sphere[7]), and types 2 and 3 (T2, T3, respectively), known as the trinuclear copper cluster (TNC) site. A distorted trigonal bipyramid of the T1 Cu site was observed in the crystal structure of the bacterial laccase-like enzyme isolated from *Bacillus subtilis* (CotA[15]), in CueO (required for copper homeostasis in *Escherichia coli*[16]), and in the small laccase (SLAC) from *Streptomyces coelicolor*.[17] The three-dimensional alignment of the C_α atoms, determined for CotA and CueO, showed a similar fold (rms deviation <2 Å).[15] Note that while the T1 copper undergoes continuous redox recycling, the TNC site reduces oxygen by an inner-sphere reaction, producing reactive and short-lived intermediate states,[18,19] as extensively studied (ref 20 and references therein). Specifically, following reduction of the T1 copper, electron transfer to the TNC by an outer-sphere intramolecular superexchange mechanism occurs.[21] Electron transfer from the T1 Cu to the TNC site over a relatively large distance (∼13 Å) is consistent with the small reorganization energies (<1 eV).[22] The long-recognized key parameter in tuning MCO behavior is however the T1 Cu potential, previously investigated for a range of applications.[1,8]

The MCOs are attractive as electrocatalysts due to the high redox potential for oxygen reduction and function at biologically benign conditions,[23] and have been integrated as oxygen reduction catalysts in numerous biofuel cell and biosensor concepts. Although recent studies of enzymatic biofuel cells[24−26] emphasized limitations of enzymes as electrocatalysts, opportunities for development were also stressed. For example, oxygen reduction using platinum catalysts in acid poses significant limitations, including partial reduction of oxygen to yield only hydrogen peroxide, or the diffusion of fuel between anode and cathode chambers, among other problems. MCOs offer advantages in catalytic specificity to effectively separate dioxygen activation and substrate oxidation.[27] However, although promising approaches for stable and efficient biocathodes were proposed, e.g., in using TvL-based[28] or CueO[29,30] immobilized on mesoporous carbon supports, there are still barriers to effective use of enzyme-modified electrodes.[31]

In particular, direct electron transfer (DET) between the redox center of MCOs and the cathode surface remains a challenge.[32] The rate of enzyme turnover is limited by interfacial electron-transfer.[33] Immobilization and "coupling" to the surface are important,[1] and the possibility of tuning the T1 redox potential could further enable improved interfacial DET. This was shown by Kamitaka et al.,[34] however not extensively confirmed as yet. Intramolecular electron transfer from the T1 copper to the TNC site could also be somewhat improved by tuning the T1 Cu potential, as was demonstrated experimentally by mutation.[34] Thus, understanding the relationship between enzyme structure-and the T1 Cu redox potential is a key component to design of engineered MCOs for efficient biofuel cells.[35] Ultimately, this will enable tuning relative to the potentials of TNC and electrode. However, computational investigation of the redox potential in MCOs has been rather limited to date.[36]

In this investigation, redox potentials and reorganization energies for a number of MCOs, including TvL,[37] CotA,[38] CueO,[30] and SLAC,[39] which vary in the experimentally measured redox potentials, were analyzed theoretically by a combination of density functional theory (DFT, quantum mechanical, QM), and computationally intensive QM/MM (molecular mechanics) molecular dynamics (MD) simulations. Calculated results demonstrated relatively good agreement with the trend observed in the experimental data, as well as insight into the effects of the coordinating environment. QM/MM MD simulations moreover provided understanding of the parameters that influence the T1 Cu potential regarding the surrounding protein and solvent beyond the close surroundings. By having an understanding of the tunability of the T1 Cu potential, a mutated SLAC enzyme was suggested for potentially improved biocathode performance. Indeed, prediction of the redox potential is of significant value to the understanding of electrochemical behavior of enzymes when employed as electrocatalysts. This work is also useful in providing a framework for applications beyond electrocatalysis, such as in molecular synthesis.[12] For example, a comparison of *Trametes vollosa* laccase (TviL) and *Myceliophthora thermophila* laccase (MtL), having potentials of 790 vs 460 mV, respectively, proved MtL to be a less effective phenol oxidase.[8] Although this is qualitatively expected (axial amino acid Phe vs Leu, respectively), subtle effects of the protein and solvent environment have to be further considered. Finally, the collective analyses of the T1 Cu redox potential of MCOs presented in this work will assist in design of efficient biocathodes by providing a framework for rational modification of the enzyme to overcome issues associated with the rate limiting step of DET.

COMPUTATIONAL DETAILS

DFT calculations were carried out at the PBE[40]/6-31+G* level, as implemented in the Gaussian software.[41] Vertical electron affinities (E_A) were calculated from energy differences between the Cu(I) and Cu(II) structures. QM/MM[42] MD simulations, as implemented in MOLARIS,[43] were applied with starting configurations that were based on the X-ray crystal structures, i.e., 1GYC for TvL,[14] 1GSK for CotA,[15]

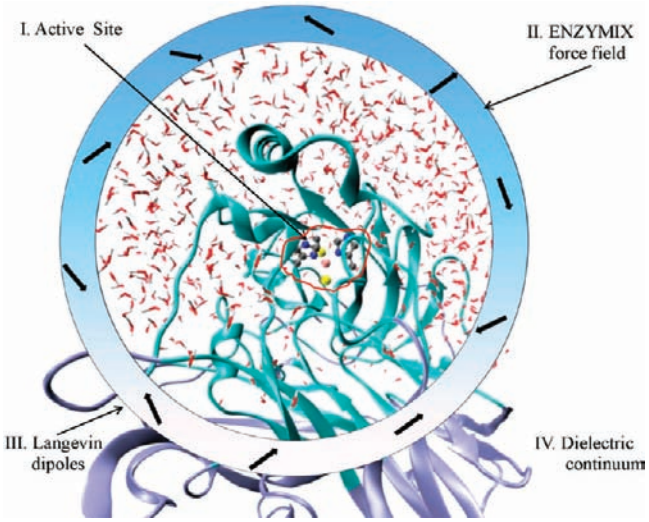

Figure 2. Model of simulated system for CueO; see description in the Computational Details section.

1KV7 for CueO,[16] and 3CG8 for SLAC.[17] The simulated system (protein and solvent) was spherical, divided into four regions. Specifically, region I comprised the T1 copper site, two His imidazole and a Cys methyl-thiolate coordinating groups, and a weakly coordinating amino acid (axial), unless noted otherwise, treated by DFT. Partial atomic charges in the QM region were obtained from ESP[44] calculations. Region II comprised of the unconstrained protein atoms and explicit water molecules up to 30 Å from the center of region I, treated by the ENZYMIX force field.[45] In region III, a 2 Å shell of Langevin dipoles, embedding region II, was added. Region IV comprised a dielectric continuum that accounts for bulk effects. The standard surface constrained all-atom solvent technique to account for the solvent,[46] and the local reaction field long-range treatment,[47] were applied. An illustration of the model (for CueO) is shown in Figure 2. In this work, we are concerned with prediction of the T1 Cu potential, given by the following:

$$\Delta E^0 = -\frac{\Delta G^0}{nF} \quad (1)$$

where ΔG^0 is the Gibbs free energy change, n number of electrons, and F Faraday's constant (0.023 kcalmol^{-1}mV^{-1}). ΔG^0 of the semireaction was calculated assuming the linear response approximation:[48]

$$\Delta G^0 = 1/2(\langle V_{red} - V_{ox}\rangle_{ox} + \langle V_{red} - V_{ox}\rangle_{red}) \quad (2)$$

where V_{red} and V_{ox} are potential energies for reduced and oxidized states, and $\langle\rangle_{ox}$ and $\langle\rangle_{red}$ represent averages over Cu(II) and Cu(I) QM/MM MD trajectories.

The structures of the MCOs considered were first relaxed and equilibrated by classical MD simulations for 100 ps with the T1 site kept fixed. Starting from well-equilibrated MD configurations, QM/MM MD simulations were carried out at 300 K with 1 fs time steps, collecting 900 snapshots. The coordinates of the T1 site were updated every 10 fs, for a total duration of 10 ps. The TNC site was kept fixed. Averages of the potential energies V were derived from trajectories of the last 9 ps of the simulations. Fluctuations in Cu-ligand bond-lengths (summarized in Table 1S of the Supporting Information) were of ca. ± 0.02 Å, and in the Cu(I) and Cu(II) energy differences of ca. ± 0.7 eV (Figure 1S of the Supporting Information). These potential energies were also used to calculate reorganization energies, as follows:

$$\lambda = 1/2(\langle V_{red} - V_{ox}\rangle_{ox} - \langle V_{red} - V_{ox}\rangle_{red}) \quad (3)$$

The sampled energy differences used in eqs 2 and 3 were well converged, with a standard error of about 0.009 eV.

RESULTS AND DISCUSSION

Calculated redox potentials by QM/MM MD simulations (mV, shifted to TvL) were 785, 577, 391, 379, for TvL, CotA, CueO, and SLAC, respectively, as compared to the experimental values (mV, vs SHE), of 785 (pH = 5.5), 455 (pH = 7.6), 477 (pH = 5), and 430 (pH = 7), for TvL, CotA, CueO, and SLAC, respectively.[37,38,30,39] In examining the T1 Cu potential, we note that compared to the low redox potential of the Cu(II) to Cu(I) reduction in aqueous solution (153 mV[49]), the relatively larger E^0 in MCOs can be attributed to the coordinating ligands, the protein environment, and the solvent.[7,22] The experimentally observed decrease in E^0 for CotA, CueO, and SLAC, as compared to TvL, was reproduced by the QM/MM MD simulations, consistent with experiment. For quantitative comparison with experimental data, pH effects have to be considered, or possible changes in the exposure to the solvent upon the enzyme's adsorption on the electrode. For example, for CueO,[30] the experimentally measured redox potential was reduced by about 80 mV for the pH range of 7−8. However, analyses of the results,

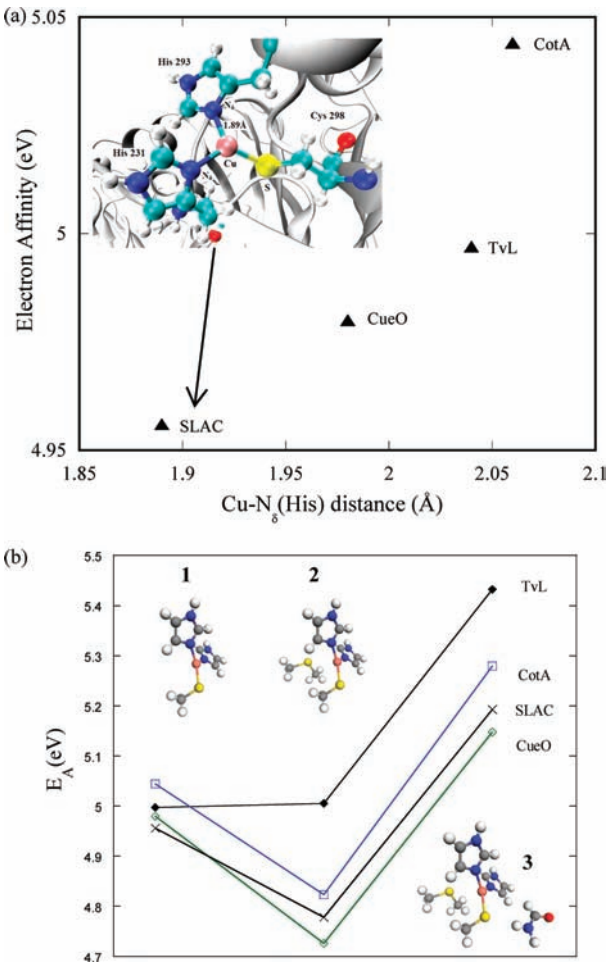

Figure 3. Calculated E_A based on the X-ray crystal structures: (a) for model compound **1** as a function of the Cu−N$_\delta$ (His) distance (shown for SLAC); (b) for model compounds **1**, **2**, and **3**. Description of the model compounds is given in the text.

dx.doi.org/10.1021/ja105586q | J. Am. Chem. Soc. 2011, 133, 4802–4809

as described in the following, provided insight into intrinsic effects on E^0.

First we considered the highly conserved immediate environment of the T1 Cu site, coordinated by His(N_δ)-Cys(S)-His-(N_δ) (model compound **1**). The distances to the T1 Cu (Å), derived from the crystal structures,[14−17] were (2.02, 2.19, 2.04), (2.05, 2.20, 2.06), (2.02, 2.19, 1.98), (2.02, 2.20, 1.89), for TvL, CotA, CueO, and SLAC, respectively. As both the CotA and SLAC MCOs' E^0 were measured at similar pH, and the axial amino acid is the same (Met), the lengthened distances to the His(N_δ) in CotA as compared to SLAC (Figure 3(a)), could be assumed to account for the somewhat larger observed redox potential. This stems from the suggestion that an elongation of the Cu−N_δ bond would result in less of a contribution of the nitrogen's lone pair, and a more electron deficient copper. Such an argument was postulated as being one of the reasons for different potentials for TvL and CcL.[14] E_A calculated values for model compounds including the minimal environment in model compound **1**, as based on the X-ray structures (see Table 1), demonstrated small variations, mostly consistent with this supposition (Figure 3(a)).

However, fluctuations due to the protein environment and solvent have to be taken into account to confirm E_A results based on crystal structures. Such subtle changes cannot be assumed from crystal structures determined at varying resolutions (1.7 Å for CotA and 2.7 Å for SLAC). Distances (Å), as derived from an average of the equilibrated QM/MM Cu(II) snapshots of the MD simulation trajectories, were (1.95, 2.12, 1.95), (1.95, 2.13, 1.95), (1.98, 2.13, 1.97), and (1.95, 2.14, 1.94), for the TvL, CotA, CueO, and SLAC, respectively (summarized in Table 1S of the Supporting Information). Bond lengths were lengthened by ca. 0.01−0.07 Å for the Cu(I) QM/MM MD-based structures (Table 1S of the Supporting Information). Note that bond lengths derived from the QM/MM MD simulations were similarly shortened for all proteins in comparison to the crystal structures. Although relative deviations for Cu−N_δ for CotA and SLAC were shown to be larger, consistent with previous work,[50] differences between the enzymes were small and inconclusive. Indeed, E_A for **1**, calculated from an average of the QM/MM MD simulation results, were similarly about 5 eV (4.96, 5.00, 5.03, 5.04, for TvL, CotA, CueO, and SLAC, respectively). Overall, relative changes in the Cu−ligand distances within the rigid His(N_δ)-Cys(S)-His(N_δ) environment around the T1 Cu site can be assumed small, having a minimal effect on the T1 Cu potential for the MCOs.

In addition to the His(N_δ)-Cys(S)-His(N_δ) coordinating ligands, the axial amino acid plays an important role in tuning the value of the T1 Cu potential, and mutation can cause relatively large changes, as has been recognized and reviewed.[1] The axial amino acids in the MCOs we examined, namely, Phe in TvL vs Met in CotA, CueO, and SLAC, shifted the potential.[51] This was demonstrated by the calculated E_A for model compounds that now include the axial amino acid (model compound **2**), as is summarized in Table 1. The relative trend of the larger E^0 for TvL as compared to the other MCOs, has been reproduced (cf. Figure 3(b)), where alteration of the axial amino acid from Phe in TvL to Met in CotA, CueO, and SLAC, reduced E_A by ca. 0.2 eV. Additionally, in comparing the trend in results of $\Delta E_A = E_A(\text{model } \mathbf{1}) - E_A(\text{model } \mathbf{2})$ for the proteins having the same axial amino acid, a smaller reduction for SLAC (Figure 2S of the Supporting Information) was noted. This is consistent with a larger Cu−S(Met) distance, of 3.45 Å (for instance vs 3.27 Å in CotA, as shown in Figure 2S of the Supporting Information). However, once again, subtle changes in a realistic environment have to be considered. The distance between the T1 Cu and the nearest heavy atom in the axial amino acid (C(Phe), S(Cys)), as derived from an average of the structures of QM/MM MD simulation trajectories, although similar for CotA, CueO, SLAC, is lengthened for TvL (Table 1S of the Supporting Information). Indeed, the electron affinities calculated from the QM/MM MD simulation results demonstrated a decrease of up to 0.16 eV (for CueO) when Phe is mutated to Met.

Table 1. E_A Vertical Electron Affinities (eV) Based on Model Compounds 1, 2, 3, As Described in the Text

	TvL	CotA	CueO	SLAC
E_A (**1**)	5.00	5.04	4.98	4.96
E_A (**2**)	5.00	4.82	4.73	4.78
E_A (**3**)	5.43	5.28	5.15	5.19

Thus, it is emphasized that the QM/MM MD simulation results captured effects of parameters that strongly influence the T1 Cu potential, which is important to consider when using such calculations as a predictive tool in future work. Our results are consistent with experimental data, upon comparing values for TvL vs CotA, CueO, and SLAC, where hydrophobic residues in the axial position were presumed to cause a higher potential. For example, in mutating the Met axial amino acid in CotA with Leu, the T1 potential was experimentally shown to increase by about 100 mV,[38] and similarly for CueO[52] and azurin.[53] In our case, using an average from the equilibrated QM/MM MD simulation results of the CotA and CueO enzymes, when the axial Met was mutated to Leu, increased E_A values indeed resulted, by 0.14 and 0.20 eV, respectively, consistent with experiment. However, Phe mutations to Leu and Met changed the redox potential from 709 to 740 mV, and 680 mV, respectively.[54,55] Tuning of the T1 Cu potential can, in part, be correlated with the axial ligand's hydrophobicity.[56]

Next, the influence of backbone atoms that form hydrogen bonds with S_{Cys} was examined (model compound **3**). The trend in values of E_A, as based on the crystal structures (see Figure 3-(b)), was not changed. However, E_A increased due to H-$(N)_{backbone}$−S_{Cys} hydrogen bonding, shown both for results based on the crystal structures and on the QM/MM MD simulation trajectories, up to 0.4 eV (Figure 3(b) and Table 1). Note that accurate prediction required QM/MM MD simulations because the H$(N)_{backbone}$−S_{Cys} distances, e.g., for SLAC, fluctuated between 2.5 and 2.9 Å, reducing ΔE_A from about 0.4 eV to ca. 0.3 eV. Respective fluctuations in the H$(N)_{backbone}$−S_{Cys} distances for TvL, CotA, and CueO, were 2.4−3.2, 2.2−3.1, 2.4−3.7 Å, respectively. Changing the local hydrogen bonding network can be considered as another additive factor for tuning the T1 Cu potential. For example, the N47S mutation in azurin perturbed the hydrogen bonding upon introduction of the hydroxyl of Ser, increasing the potential by about 130 mV, while F114P deletes a direct hydrogen bond to the Cys amino, resulting in a lower redox potential by about 90 mV.[55]

Beyond the T1 Cu coordination sphere, the protein dipole may affect the redox potential.[57] For example, it was shown that the ∼20 Å Ala53-Ser66 α helix in azurin from *Pseudomonas aeruginosa*, with a dipole that is approximately parallel to the direction of the axial ligand, decreased the redox potential by a significant amount.[58] To discern the influences of the protein main-chain, side-chain, and solvent dipoles on the T1 Cu potential for the

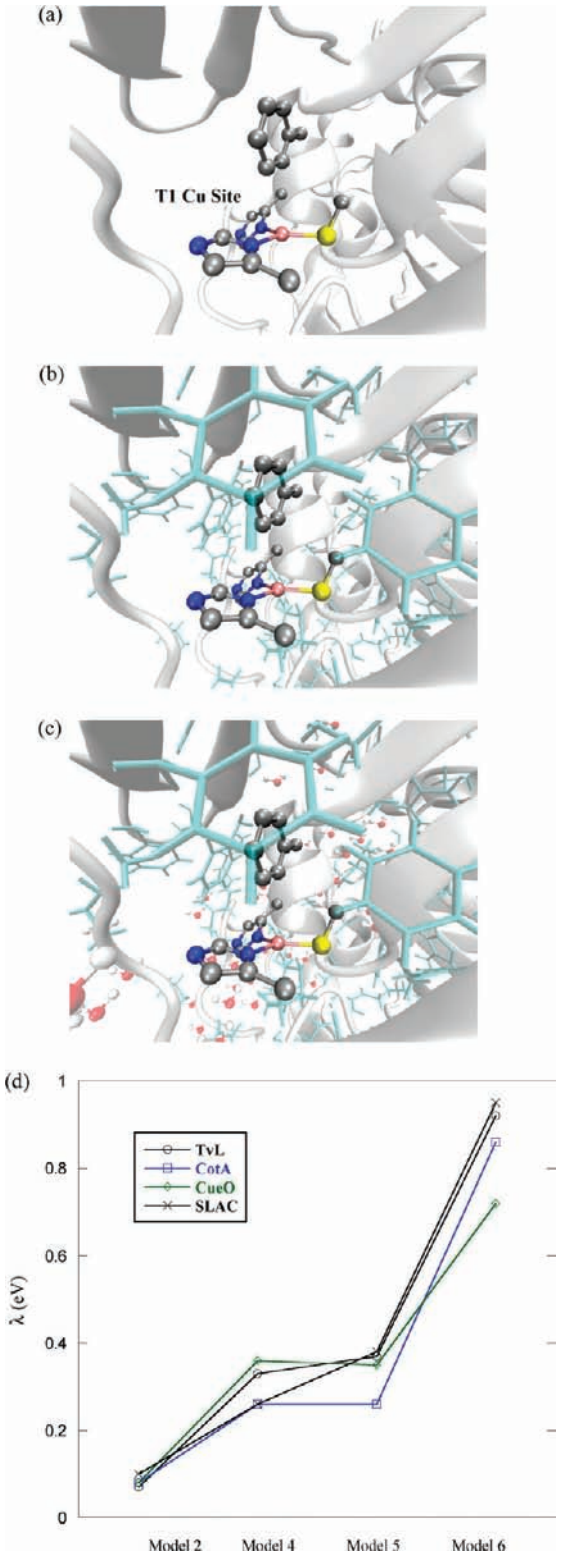

Figure 4. Description of model compounds, including: (a) **4**, protein backbone dipoles; (b) **5**, protein backbone and side-chain dipoles; (c) **6**, protein dipoles and solvent dipoles; the His(N_δ)-Cys(S)-His(N_δ) environment of the T1 Cu site is explicitly shown; and (d) effects of the protein and solvent environment on the reorganization energies of the 4 MCOs.

MCOs we considered, electron affinities of four model systems were analyzed. Specifically, model compound **2** was compared to model compounds **4**−**6** (shown in Figures 4(a)−(c)), including the protein backbone (model compound **4**), protein (model compound **5**) and protein and solvent (model compound **6**). E_A of **2** was calculated at the DFT level, while results for model compounds **4**, **5**, and **6**, were derived from averages QM/MM MD simulations, as summarized in Table 2.

Table 2. Calculated Average E_A Values of the T1 Copper Site (Model Compound 2), Using Selected Configurations from Cu(II) QM/MM MD Simulation Trajectories, Based on 300 Configurations [a,b]

	TvL	CotA	CueO	SLAC
E_A (**2**)	4.99	4.82	4.81	4.85
ΔE_A (**4**)	0.41	0.86	0.05	1.59
ΔE_A (**5**)	0.17	0.43	−0.31	0.54
ΔE_A (**6**)	−1.05	−1.06	−1.08	−1.32

[a] Standard errors were ≤0.001, 0.007, 0.010, 0.015, for model compounds **2**, **4**, **5**, and **6**, respectively. [b] ΔE_A are shifts relative to results for **2**, as dependent on incremental inclusion of dipoles of the protein backbone (model compound **4**), protein dipoles (model compound **5**), and both protein and solvent dipoles (model compound **6**), as shown in Figure 4.

As the SLAC enzyme has a low sequence similarity with other MCOs, we first compared effects of the protein backbone and side-chains on the electron affinities for the enzymes TvL, CotA, and CueO. Side-chain dipoles, namely (ΔE_A(**4**)−ΔE_A(**5**), see Table 2), have shown reduction of E_A by 0.2, 0.4, and 0.4 eV for TvL, CotA, and CueO, respectively, clearly smaller for the TvL MCO. Indeed, in addition to the coordinating ligands, another contribution to the larger potential of TvL could stem from the protein side-chains' dipole, as yet not explored. Influence of the solvent was relatively similar for the three proteins. However, the SLAC enzyme demonstrated differences. Specifically, the protein backbone dipole increased E_A by a relatively larger value, of 1.6 eV, and a relatively larger reduction of the potential, as dependent on the protein's side-chain dipoles, was noted. In addition, ΔE_A for the solvent dipoles for the TvL, CotA, and CueO enzymes, of 1.2, 1.5, and 0.77 eV, respectively, were smaller than for the SLAC, for which a larger decrease was noted (1.9 eV), indicating a different degree of exposure to solvent.[50,57] Interestingly, (E_A(**2**) + E_A(**6**)) values were shown to be consistent with the experimental redox potentials. Overall, it was shown that the backbone dipoles in the MCOs increased the redox potential while the side-chain and solvent dipoles decreased it.

QM/MM MD simulations provided insight also into effects on the reorganization energies λ. Calculated λ were 0.9, 0.8, 0.7, and 0.9 eV, for the TvL, CotA, CueO, and SLAC MCOs, respectively, for the Cu T1 site environment. The results are somewhat overestimated,[22,59] possibly due to inadequacy of the QM region. However, in comparing λ from QM rather than QM/MM MD simulation energy values, of ca. 0.1 eV for TvL, CotA, CueO, and SLAC, it was demonstrated that reorganization energies for the T1 Cu were dominated by the protein backbone, and moreover solvent rearrangements (see Figure 4(d)), thus providing understanding of contributions to λ.

Regarding applications, in designing for efficient DET in a biocathode, the adsorption on the electrode of the enzyme's binding site is of interest. Notably, the CotA MCO has a larger solvent accessible site, and molecular surface and volume, than the TvL and CueO enzymes.[14,15] Specifically, the TvL's structure exhibits a small negatively charged cavity about 6.5 Å from the T1

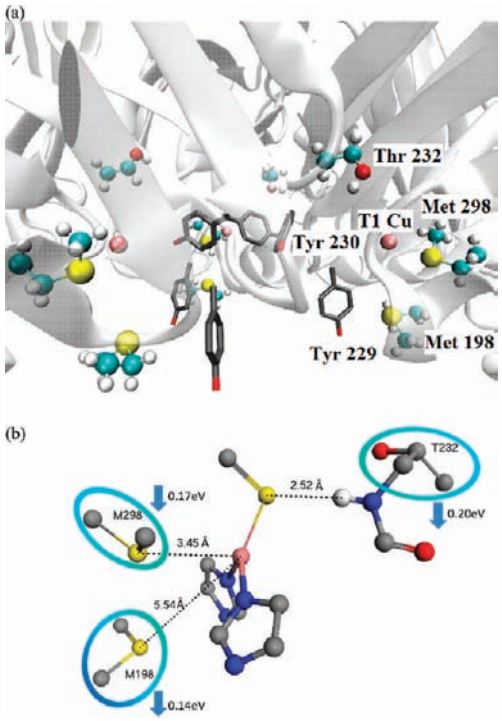

Figure 5. The enzyme SLAC's (a) hydrophobic binding pocket, showing suggested amino acids for mutation; (b) E_A based on the X-ray crystal structure[17] for various model compounds of SLAC. The blue circles show the portion that was included in the E_A calculations.

site for binding the substrate, while CotA has a distinctive structure of a flexible lid-like region proximate to the substrate-binding site to aid substrate accessibility. CueO[16] contains a Met-rich helix (a.a. 356−371 with seven Met residues) and a loop (a.a. 372−379 with two Met residues) lying over the T1 copper site in the third domain, likely involved in homeostasis in bacteria, but which may hinder substrate access. Compared to these MCOs, the SLAC's substrate binding site may present advantages for adsorption on a solid electrode. As described by Skálová et al.,[17] the trimeric organization of the MCO and relative closeness of the T1 Cu bring the three binding sites into proximity, offering additional adsorption sites. The T1 binding site is relatively close to the surface, but more importantly, two consecutive residues in the sequence, Tyr229 and Tyr230, form a major part of the shallow pocket, which may allow facile adsorption on a carbon electrode, possibly upon chemical modification, as previously carried out.[28] Other hydrophobic residues also comprise the binding pocket, as shown in Figure 5(a). However, mutations of SLAC for an increased T1 Cu potential will have to be considered for fabricating an efficient biocathode.

Our calculations demonstrated that although QM/MM MD simulations are required for a careful analysis of the parameters that affect the T1 Cu redox potential in a realistic environment, reasonable suppositions can be drawn from model compounds of the crystal structures. E_A calculated results, as based on the crystal structure of the SLAC MCO model compounds, have shown that the proximate Met198 and Thr232 resulted in E_A decreases of 0.14 and 0.20 eV, respectively (Figure 5(b)). Thus, in addition to the axial ligand Met298, mutations of Met198 and Thr232 can potentially increase the redox potential. However, future experimental and QM/MM MD simulations have to be carried out to quantify details of the effects of the environment, which, in turn, will result in improved performance. For example, in further assessment of such mutations, MD trajectories' analyses were utilized, which have shown that the $H(N)_{backbone}-S_{Cys}$ distances in SLAC fluctuated between 2.5 and 2.9 Å. Three configurations, with distances of 2.50, 2.70, and 2.92 Å, respectively, were selected, and Thr232 was mutated to Val. The resulting increase of E_A, of about 0.1 eV, clearly demonstrated a larger expected T1 Cu potential. Similarly, Cu−S(Met198) fluctuated between 4.7 and 5.7 Å, and selected configurations with distances of 4.71,5.20, 5.70 Å, respectively, mutating Met198 to Leu, resulting in an increase in E_A of about 0.1 eV. Thus, it is expected that the mutated SLAC enzymes, namely, T232 V and M198L, will result in a higher potential, but full confirmation by QM/MM MD simulations for the mutated proteins is to be carried out in future work. Other mutations will also be considered in future work, e.g., for Asp 206 in TvL; Ala and Gln keep or raise the biocatalytic activity and shift the optimal pH for some substrates.[60] However, mutating Glu498 in CotA with Thr or Leu impaired the biocatalytic activity.[61] Finally, note that experimental elucidation of the oxygen reduction mechanism was recently further attempted for the TvL[62] and SLAC enzymes,[63] and also intramolecular electron transfer enhancement,[64] to be examined in future work.

CONCLUSIONS

The T1 Cu redox potentials and reorganization energies for TvL, CotA, CueO, and SLAC, were calculated by combining DFT and QM/MM MD simulations. The results agreed well with experimentally measured values. Computational prediction of the T1 Cu redox potential in MCOs has previously been rather limited, often to gas state calculations.[50] However, long-range effects of the protein can be important,[55,57] as carried out in this work. The trend in the T1 Cu redox potentials was reasonably reproduced by the QM/MM MD simulations. Discrepancies could be addressed by using a larger QM region, however such an approach is currently computationally prohibitive. Furthermore, in examining the effects of the immediate T1 Cu site environment, we have shown that the highly conserved coordination of $His(N_\delta)$-Cys(S)-$His(N_\delta)$ surrounding the T1 Cu site has had little influence on the potential. This was demonstrated upon analyses of the equilibrated structures from QM/MM MD simulation trajectories, which take into account the realistic protein and solvent environment. However, the nature of the axial amino acid strongly impacted the potential, decreasing it upon varying Phe in TvL to Met. The QM/MM MD simulation results reproduced a larger T1 Cu potential for TvL, having a hydrophobic axial amino acid. Local changes of the hydrogen bonding of $H(N)_{backbone}-S_{Cys}$, which could affect the increase of the T1 potential, were additionally analyzed.

Beyond the T1 Cu coordination sphere, the QM/MM MD simulation results discerned effects of the protein and solvent environment. It was demonstrated that the backbone dipoles in the MCOs increased the redox potential while the side-chain and solvent dipoles decreased it. Moreover, different solvent effects for SLAC were explained. By having an estimate of the tunability of the T1 Cu potential, and as a relatively high cathodic redox potential can be achieved with Cu in a well-defined protein environment, a mutated MCO was proposed for improved performance, which has not been previously suggested. The mutated enzyme will be used for modeling the physisorption characteristics on the bioelectrode in future work.

■ ASSOCIATED CONTENT

Supporting Information. Cu−ligand distances (Å), and average values of energy differences (eV) from QM/MM MD simulations, for TvL, CotA, CueO, and SLAC. Changes in the electron affinity (eV) for CotA, CueO, and SLAC as a function of Cu−S(Met) distance (Å). Listed authors of ref 41. This material is available free of charge via the Internet at http://pubs.acs.org.

■ AUTHOR INFORMATION

Corresponding Author
Ruth.Pachter@wpafb.af.mil

■ ACKNOWLEDGMENT

We gratefully acknowledge support from the Air Force Office of Scientific Research, and helpful assistance from the AFRL DSRC for High Performance Computing. A. Warshel and his group are acknowledged for a version of the MOLARIS software package and helpful discussion. The referees are gratefully acknowledged for excellent comments.

■ REFERENCES

(1) Rodgers, C. J.; Blanford, C. F.; Giddens, S. R.; Skamnioti, P.; Armstrong, F. A.; Gurr, S. J. *Trends Biotechnol.* **2010**, *28*, 63–72.
(2) Giardina, P.; Faraco, V.; Pezzella, C.; Piscitelli, A.; Vanhulle, S.; Sannia, G. *Cell. Mol. Life Sci.* **2010**, *67*, 369–385.
(3) Solomon, E. I.; Hare, J. W.; Gray, H. B. *Proc. Natl. Acad. Sci.* **1976**, *73*, 1389–1393.
(4) Solomon, E. I.; Sundaram, U. M.; Machonkin, T. E. *Chem. Rev.* **1996**, *96*, 2563–2606.
(5) Kosman, D. J. *J. Biol. Inorg. Chem.* **2010**, *15*, 15–28, and references therein.
(6) Zhukhlistova, N. E.; Zhukova, Yu. N.; Lyashenko, A. V.; Zaitsev, V. N.; Mikhailov, A. M. *Crystallogr. Rep.* **2008**, *53*, 92–109.
(7) Battistuzzi, G.; Bellei, M.; Leonardi, A.; Pierattelli, R.; Candia, A.; Vila, A. J.; Sola, M. *J. Biol. Inorg. Chem.* **2005**, *10*, 867–873.
(8) Tadesse, M. A.; D'Annibale, A.; Galli, C.; Gentili, P.; Sergi, F. *Org. Biomol. Chem.* **2008**, *6*, 868–878.
(9) Baldrian, P. *FEMS Microbiol. Rev.* **2006**, *30*, 215–242.
(10) Sharma, P.; Goel, R.; Capalash, N. *World J. Microbiol. Biotechnol.* **2007**, *23*, 823–832.
(11) Claus, H. *Micron* **2004**, *35*, 93–96.
(12) Mikolasch, A.; Schauer, F. *Appl. Microbiol. Biotech.* **2009**, *82*, 605–624.
(13) Martinez, A. T.; Ruiz-Duenas, F. J.; Martinez, M. J.; del Rio, J. C.; Gutierrez, A. *Curr. Opin. Biotechnol.* **2009**, *20*, 348–357.
(14) Piontek, K.; Antorini, M.; Choinowski, T. *J. Biol. Chem.* **2002**, *277*, 37663–37669.
(15) Enguita, F. J.; Martins, L. O.; Henriques, A. O.; Carrondo, M. A. *J. Biol. Chem.* **2003**, *278*, 19416–19425.
(16) Roberts, S. A.; Weichsel, A.; Grass, G.; Thakali, K.; Hazzard, J. T.; Tollin, G.; Rensing, C.; Montfort, W. R. *Proc. Natl. Acad. Sci.* **2002**, *99*, 2766–2771.
(17) Skálová, T.; Dohnálek, J.; Østergaard, L. H.; Østergaard, P. R.; Kolenko, P.; Dusková, J.; Stepánková, A.; Hasek, J. *J. Mol. Biol.* **2009**, *385*, 1165–1178.
(18) Sakurai, T.; Kataoka, K. *Chem. Rec.* **2007**, *7*, 220–229.
(19) Solomon, E. I.; Augustine, A. J.; Yoon, J. *Dalton Trans.* **2008**, 3921–3932.
(20) Yoon, J.; Fujii, S.; Solomon, E. I. *Proc. Natl. Acad. Sci.* **2009**, *106*, 6585–6590. Bukh, C.; Lund, M.; Bjerrum., J. *Inorg. Biochem.* **2006**, *100*, 1547–1557.
(21) Zhang, J.; Kuznetsov, A. M.; Medvedev, I. G.; Chi, Q.; Albrecht, T.; Jensen, P. S.; Ulstrup, J. *Chem. Rev.* **2008**, *108*, 2737–2791.
(22) Gray, H. B.; Malmström, B. G.; Williams, R. J. P. *J. Biol. Inorg. Chem.* **2000**, *5*, 551–559.
(23) Soukharev, V.; Mano, N.; Heller, A. *J. Am. Chem. Soc.* **2004**, *126*, 8368–8369.
(24) Bullen, R. A.; Arnot, T. C.; Lakeman, J. B.; Walsh, F. C. *Biosens. Bioelectron.* **2006**, *21*, 2015–2045.
(25) Cracknell, J. A.; Vincent, K. A.; Armstrong, F. A. *Chem. Rev.* **2008**, *108*, 2439–2461.
(26) Willner, I.; Yan, Y.-M.; Willner, B.; Tel-Vered, R. *Fuel Cells* **2009**, *1*, 7–24.
(27) Gewirth, A. A.; Thorum, M. S. *Inorg. Chem.* **2010**, *49*, 3557–3566.
(28) Blanford, C. F.; Heath, R. S.; Armstrong, F. A. *Chem. Commun.* **2007**, 1710–1712. Blanford, C. F.; Foster, C. E.; Heath, R. S.; Armstrong, F. A. *Faraday Discuss.* **2008**, *140*, 319–335.
(29) Miura, Y.; Tsujimura, S.; Kamitaka, Y.; Kurose, S.; Kataoka, K.; Sakurai, T.; Kano, K. *Chem. Lett.* **2007**, *36*, 132–133.
(30) Miura, Y.; Tsujimura, S.; Kurose, S.; Kamitaka, Y.; Kataoka, K.; Sakurai, T.; Kano, K. *Fuel Cells* **2009**, *9*, 70–78.
(31) Davis, F.; Higson, S. P. J. *Biosens. Bioelectron.* **2007**, *22*, 1224.
(32) Ivnitski, D.; Artyushkova, K.; Atanassov, P. *Bioelectrochem.* **2008**, *74*, 101–110.
(33) Reda, T.; Hirst, J. *J. Phys. Chem. B* **2006**, *110*, 1394–1404.
(34) Kamitaka, Y.; Tsujimura, S.; Kataoka, K.; Sakurai, T.; Ikeda, T.; Kano, K. *J. Electroanal. Chem.* **2007**, *601*, 119–124.
(35) Kennedy, M. L.; Gibney, B. R. *Curr. Opin. Struct. Biol.* **2001**, *11*, 485–490.
(36) Ryde, U.; Olsson, M. H. M. *Int. J. Quantum Chem.* **2001**, *81*, 335–347.
(37) Reinhammar, B. *Biochim. Biophys. Acta* **1972**, *275*, 245–259.
(38) Durão, P.; Bento, I.; Fernandes, A. T.; Melo, E. P.; Lindley, P. F.; Martins, L. O. *J. Biol. Inorg. Chem.* **2006**, *11*, 514–526.
(39) Gallaway, J.; Wheeldon, I.; Rincon, R.; Atanassov, P.; Banta, S.; Barton, S. C. *Biosens. Bioelectron.* **2008**, *23*, 1229–1235.
(40) Perdew, J. P.; Burke, K.; Ernzerhof, M. *Phys. Rev. Lett.* **1996**, *77*, 3865.
(41) Frisch, M. J.; et al. , Gaussian, Inc., Wallingford CT, 2009.
(42) (a) Warshel, A.; Levitt, M. *J. Mol. Biol.* **1976**, *103*, 227–249. (b) Gao *J. Acc. Chem. Res.* **1996**, *29*, 298–305. (c) Friesner, R.; Beachy, M. D. *Curr. Opin. Struct. Biol.* **1998**, *8*, 257–262. (d) Monard, G.; Merz, K. M. *Acc. Chem. Res.* **1998**, *32*, 904–911. (e) Zhang, Y.; Liu, H.; Yang, W. *J. Chem. Phys.* **2000**, *112*, 3483–3492. (f) Field, M. *J. Comput. Chem.* **2002**, *23*, 48–58.
(43) Chu, Z. T.; Villa, J.; Strajbl, M.; Schutz, C. N.; Shurki, A.; Warshel, A.; MOLARIS 9.05 ed.; University of the Southern California: Los-Angeles, 2004.
(44) Singh, U. C.; Kollman, P. A. *J. Comput. Chem.* **1984**, *5*, 129–145. Besler, B. H.; Merz, K. M.; Kollman, P. A. *J. Comput. Chem.* **1990**, *11*, 431–439.
(45) Lee, F. S. L.; Chu, Z. T.; Warshel, A. *J. Comput. Chem.* **1993**, *14*, 161–185.
(46) Warshel, A.; King, G. *Chem. Phys. Lett.* **1985**, *121*, 124–129.
(47) King, G.; Warshel, A. *J. Chem. Phys.* **1990**, *93*, 8682–8692.
(48) (a) Warshel, A. *J. Phys. Chem.* **1982**, *86*, 2218. (b) Blumberger, J.; Tavernelli, I.; Klein, M. L.; Sprik, M. *J. Chem. Phys.* **2006**, *124*, 064507–12.
(49) Cotton, F. A.; Wilkinson, G.; Murilloand, M. C. A. *Advanced Inorganic Chemistry*; Wiley: New York: 1999.
(50) Li, H.; Webb, S. P.; Ivanic, J.; Jensen, J. H. *J. Am. Chem. Soc.* **2004**, *126*, 8010–8019.
(51) Holm, R. H.; Kennepohl, P.; Solomon, E. I. *Chem. Rev.* **1996**, *96*, 2239–2314.
(52) Sakurai, T.; Kataoka, K. *Cell. Mol. Life Sci.* **2007**, *64*, 2642–2656.
(53) Berry, S. M.; Ralle, M.; Low, D. W.; Blackburn, N. J.; Lu, Y. *J. Am. Chem. Soc.* **2003**, *125*, 8760–8768.
(54) Xu, F.; Palmer, A. E.; Yaver, D. S.; Berka, R. M.; Gambetta, G. A.; Brown, S. H.; Solomon, E. I. *J. Biol. Chem.* **1999**, *274*, 12372–12375.

(55) Marshall, N. M.; Garner, D. K.; Wilson, T. D.; Gao, Y.-G.; Robinson, H.; Nilges, M. J.; Lu, Y. *Nature* **2009**, *462*, 113–116.
(56) Wimley, W. C.; White, S. H. *Nat. Struct. Biol.* **1996**, *3*, 842–848.
(57) Olsson, M. H. M.; Hong, G.; Warshel, A. *J. Am. Chem. Soc.* **2003**, *125*, 5025–5039.
(58) Cascella, M.; Magistrato, A.; Tavernelli, I.; Carloni, P.; Rothlisberger, U. *Proc. Natl. Acad. Sci.* **2006**, *103*, 19641.
(59) Di Bilio, A. J.; Hill, M. G.; Bonander, N.; Karlsson, B. G.; Villahermosa, R. M.; Malmstrom, B. G.; Winkler, J. R.; Gray, H. B. *J. Am. Chem. Soc.* **1997**, *119*, 9921–9922.
(60) Madzak, C.; Mimmi, M. C.; Caminade, E.; Brault, A.; Baumberger, S.; Briozzo, P.; Mougin, C.; Jolivalt, C. *Protein Eng. Des. Sel.* **2006**, *19*, 77–84.
(61) Chen, Z.; Durão, P.; Silva, C. S.; Pereira, M. M.; Todorovic, S.; Hildebrandt, P.; Bento, I.; Lindley, P. F.; Martins, L. O. *Dalton Trans.* **2010**, *39*, 2875–82.
(62) Matijosyte, I.; Arends, I. W. C. E.; Sheldon, R. A.; de Vries, S. *Inorg. Chim. Acta* **2008**, *361*, 1202–1206.
(63) Tepper, A. W. J. W.; Milikisyants, S.; Sottini, S.; Vijgenboom, E.; Groenen, E. J. J.; Canters, G. W. *J. Am. Chem. Soc.* **2009**, *131*, 11680–11682.
(64) Farver, O.; Tepper, A. W. J. W.; Wherland, S.; Canters, G. W.; Pecht, I. *J. Am. Chem. Soc.* **2009**, *131*, 18226–18227.